ISSN: 2754-4753

Journal of Physics & Optics Sciences

SCIENTIFIC Research and Community

Research Article

Open Access

Effects of Heat Treatment on some Magnetic Properties of Amorphous Alloys Containing $Fe_{49}Ni_{29}Si_9B_{13}$ and $Fe_{59}Ni_{19}Si_9B_{13}$

Rafiyev NM

Azerbaijan University of Architecture and Construction, Baku, AZ1073 Azerbaijan

ABSTRACT

The effect of various processing modes on the magnetic properties of amorphous $Fe_{49}Ni_{29}Si_9B_{13}$ and $Fe_{59}Ni_{19}Si_9B_{13}$ alloys obtained by melt spinning was examined. Samples from both alloys were prepared separately in the magnetic field and without the field. An increase in soft magnetic properties was observed during the period of the transition to the crystalline phase, (H_c = 50 A/m, B_r = 2.16 Tl). After crystalline phases are formed, materials lose their soft magnetic properties.

The composition of samples of rapidly cooled various Fe and Ni containing alloys were tested on XRD. Shimadzu XRD 6000 diffractometer was used to determine the phases of amorphous alloys by applying Cu Ka radiation at 40 kV/30 mA (CuKa1 = 122.59 A/m). Kβ radiation is eliminated by graphite monochromator.

***Corresponding author**

Rafiyev NM, Azerbaijan University of Architecture and Construction, Baku, AZ1073 Azerbaijan. Email: nrafiyev@mail.ru

Received: April 29, 2022; **Accepted:** May 05, 2022; **Published:** May 12, 2022

Keywords: Amorphous, Magnetic, Alloy, Processing

Introduction

Numerous studies have been conducted on the influence of external factors on the magnetic properties of amorphous alloys containing Fe-Ni-Si-B, and these studies continue to this day. There are many effects that can change the properties of these alloys, the main of which are thermal effects and the chemical composition of the material. The effects of the stress relieving process on the magnetic parameters and the dependence of the magnetization on the complex processing modes were determined [1-2]. The magnetic properties are significantly affected by even a small change in the amount of elements in the chemical composition. For example, it is known that an increase in Ni in a 30% FeNi alloy does not reduce the sensitivity to anisotropy and correction force [3-7]. Particular interest is the reshaping of the structure of the samples without breaking the amorphous phase as a result of the influence of different processing regimes and the changes that occur in the magnetic properties at this stage. For example, in $Fe_{45}Co_{45}Ni_{10}$ alloy, a significant decrease in the coercive force is felt when the size of the grains formed at this stage is in the order of 10nm [4-8].

This article examines changes in the structure of amorphous materials of exact composition as a result of heat, chemical composition and other external influences, and the final effects of these changes on the magnetic properties.

Experimental Materials and Methods

The starting used materials are manufactured by Sigma Aldrich, with a purity of 99.99%. From the mentioned elements, alloys of the specified composition by Melt spinning method were obtained in the form of bands with a thickness of 25 micron.

The composition of various Fe and Ni metal alloy samples which is rapidly cooled was analyzed by XRD test. Shimadzu XRD 6000 diffractometer was used to determine the phases of amorphous alloys in copper radiation at 40 kV and 30 mA (CuKa1=122.59 A/m). Kβ radiation is eliminated by a graphite monochromator.

The DSC curves of the alloys were drawn on a DSC/60-60A differential scanning calorimeter manufactured by Shimadzu.

Microscopic images of the tapes were taken on a Hitachi S-3400N Scanning Electron Microscope (SEM) manufactured by Hitachi.

Measurement of magnetic parameters was carried out on a vibrating magnetometer EZ-VSM with the highest electromagnetic base up to 3 Tl.

Analysis of Experiment

As shown in Figure 1, when the alloys containing $Fe_{49}Ni_{29}Si_9B_{13}$ and (a) and $Fe_{59}Ni_{19}Si_9B_{13}$ (b). are subjected to slow cooling at 450°C for 40 minutes, no crystalline phase peaks are observed in the XRD analysis spectrum, and thus the whole phase is amorphous.

However, some simple peaks between 40° and 50° are observed in the XRD spectrum of alloys, which are associated with the formation of metastable phases in that range.

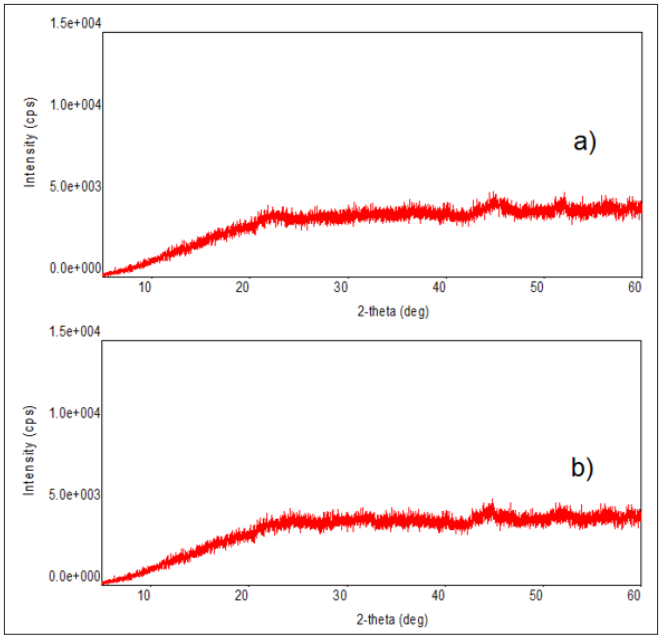

Figure 1: XRD spectra of alloys containing $Fe_{49}Ni_{29}Si_9B_{13}$ and (a) and $Fe_{59}Ni_{19}Si_9B_{13}$ (b).

Figure 2 shows the SEM spectra of the initial stage of crystallization of amorphous alloys containing $Fe_{49}Ni_{29}Si_9B_{13}$ (a) and $Fe_{59}Ni_{19}Si_9B_{13}$ (b). It is clear from the SEM spectra that these alloys consist of amorphous layers that contain agglomerated irregular particles and small voids in the structure. It is believed that, these agglomerations have been formed by the forces of Van der Waals.

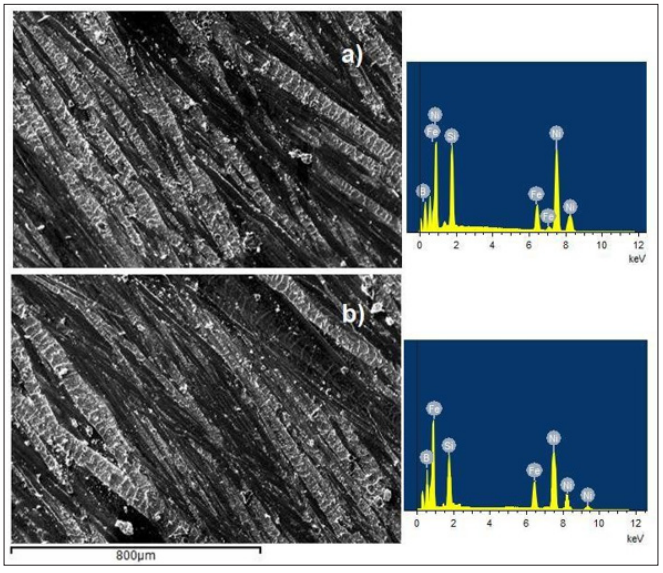

Figure 2: SEM spectra of alloys containing $Fe_{49}Ni_{29}Si_9B_{13}$ (a) and $Fe_{59}Ni_{19}Si_9B_{13}$ (b).

In addition, small crystalline particles of 366-604 nm are observed (Figure 3). These tiny particles collide with other particles due to the loss of kinetic energy during the cooling process, and because of the short period during these collisions, particles freeze between each other. The size of these irregular shapes is in the range of about 300-600 nm. As a result, when amorphous phases occur, unchangeable metaphases and intermetallic phases appear over their whole surface in a more regular at some extent and mostly irregular and spherical shape.

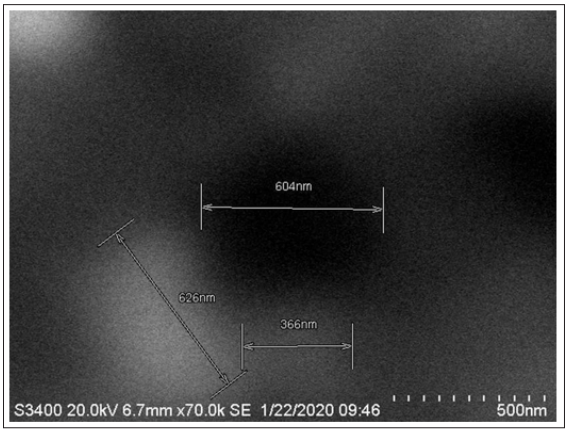

Figure 3: SEM image at 70,000 times magnification of a sample containing $Fe_{49}Ni_{29}Si_9B_{13}$

Figure 4 shows the DSC spectra of alloys containing $Fe_{49}Ni_{29}Si_9B_{13}$ in $Fe_{59}Ni_{19}Si_9B_{13}$ alloy.

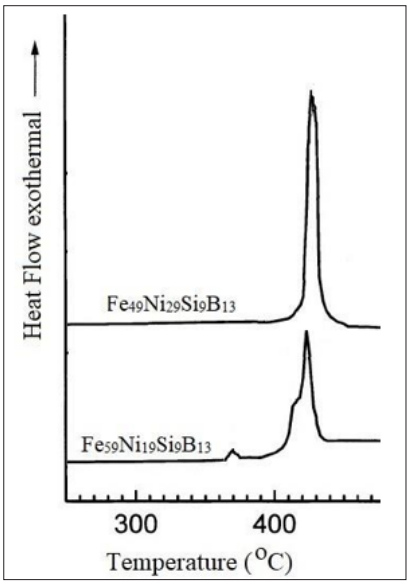

Figure 4: DSC spectra of alloys containing $Fe_{49}Ni_{29}Si_9B_{13}$ in $Fe_{59}Ni_{19}Si_9B_{13}$ alloy

As can be seen, these two alloys with different compositions have exothermic peaks that overlap in the curves of the metal alloys. A comparison of these DSC spectra reveals that only one peak is observed in the DSC spectrum of $Fe_{49}Ni_{29}Si_9B_{13}$ alloy at 420°C. However, in the DSC spectrum of metal alloys containing $Fe_{59}Ni_{19}Si_9B_{13}$, in addition to the main peak observed at 420°C, additional small peaks are observed at 370°C and 410°C, which leads to the formation of negligible crystalline phases at these temperatures in alloys with high percentage of iron. The effect of these crystalline phases on the magnetic properties of metal alloys is described in more detail in the following paragraphs. It can be concluded that the crystallization temperature of the two presented metal alloys depends on their composition. İn order to study the crystallization properties of these two samples, it is needed to study them at slow cooling temperatures.

Figure 5 shows the temperature dependence of the maximum magnetic permeability (Bm) of $Fe_{49}Ni_{29}Si_9B_{13}$ and $Fe_{59}Ni_{19}Si_9B_{13}$ alloys in different processing modes.

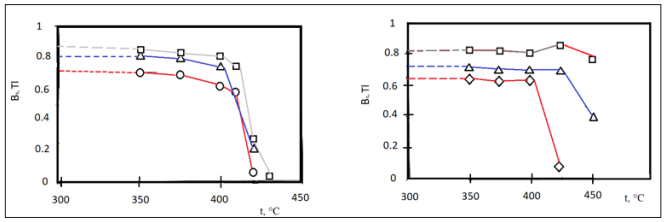

Figure 5: Influence of processing modes and processing temperature on the maximum magnetic induction of $Fe_{49}Ni_{29}Si_9B_{13}$ and $Fe_{59}Ni_{19}Si_9B_{13}$ alloys.

o- Initial sample, □ - prepared in a magnetic field, Δ- stress relieving

Thus, the annealing and processing in the magnetic field in both alloys lead to an improvement in the magnetic properties. Relatively higher values (0.9 Tl) are observed in samples taken at the beginning of the annealing and processing in the magnetic field.

As can be seen from the figure, there is a sharp drop in the value of the maximum magnetic permeability Bm at 420°C. This is due to the transition of the amorphous phase to the crystalline phase at this temperature. However, a drop of this figure occurs later in the $Fe_{59}Ni_{19}Si_9B_{13}$ alloy than in the $Fe_{49}Ni_{29}Si_9B_{13}$ alloy by 20°C. This demonstrates that a high concentration of iron atoms causes an increase in the crystalline phase transition temperature.

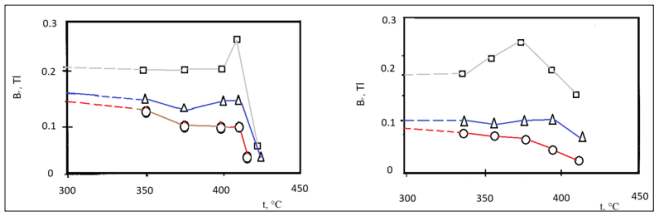

Figure 6: Influence of processing modes and processing temperature on residual magnetization of $Fe_{49}Ni_{29}Si_9B_{13}$ and $Fe_{59}Ni_{19}Si_9B_{13}$ alloys.
o- Initial sample □ - processed in a magnetic field, Δ- stress relieving

In the sample processed in the magnetic field, an increase in the value of residual magnetic induction (B_r) is observed at different temperatures ($Fe_{59}Ni_{19}Si_9B_{13}$ -370°C, $Fe_{49}Ni_{29}Si_9B_{13}$ -420°C) before the formation of crystalline phases, but the B_r value decreases sharply if process is continued. Such a sharp drop in the value of B_r coincides with the formation of crystalline phases, as can be seen from the DSC curves. This gives us basis to say that with the formation of crystalline phases in the studied samples the magnetic soft properties are being reduced. However, at the beginning of the crystallization phase, when the first fine-grained crystalline particles are formed (Figure 3), the best magnetic-soft properties are observed in this studied material (B_r = 2.16Tl). According to the theory of the directional atomic pair ordering (Néeyel- Taniguchi theory), when a system is thermally activated and becomes under the influence of an external magnetic field, the atomic pairs are arranged in such a way that their total magnetic energy becomes minimal [6-10]. After that, when the system is cooled to a low temperature, ie until the diffusion of atoms is stopped, the orientation of the atomic pairs almost freezes. As a result, magnetic anisotropy is formed in the system. Based on the theory of the directional atomic pair ordering, the increase in B_r before crystallization can be explained. When the sample is processed by slow cooling in a magnetic field for 40 min, an axially oriented magnetic anisotropy starts to appear, as shown in, which leads to an increase in the value of B_r [5].

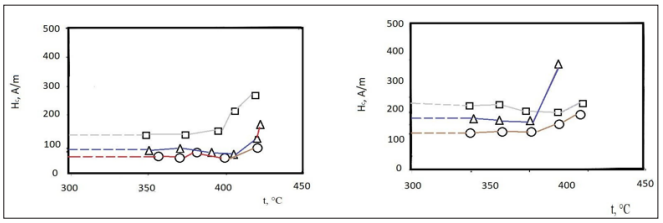

Figure 7: Influence of processing modes and processing temperature on hysteresis loop parameters of $Fe_{49}Ni_{29}Si_9B_{13}$ and $Fe_{59}Ni_{19}Si_9B_{13}$ alloys.
o- Initial sample □ - processed in a magnetic field, Δ- stress relieving

The coercive force (Hc) does not change till the formation of the crystalline phase, after which it rises. Hc is noticed only in the stress relieving sample a sharp increase at 400°C. Thus, the change in Hc also depends on the degree of crystallization of the material.

Conclusion

Amorphous samples containing $Fe_{49}Ni_{29}Si_9B_{13}$ and $Fe_{59}Ni_{19}Si_9B_{13}$ were thermally processed in a magnetic field and in a fieldless state at a temperature of 450-500°C by slow cooling for 40 minutes. It is clear from the SEM images that the grains are 300-600nm in size when the initial crystalline phases are formed. Images of DSC curves in both alloys show that a peak is observed at 420°C in $Fe_{49}Ni_{29}Si_9B_{13}$ alloy and two peaks at 370-410°C in $Fe_{59}Ni_{19}Si_9B_{13}$ alloy. These peaks indicate the initial formation of crystals. In both samples, the value of magnetic induction Bm and B_r is higher when processed in a magnetic field (Bm≈1Tl, B_r≈2.16Tl). The value of magnetic induction of Bm and B_r rises when a fine-grained (300-600nm) structure is formed in the initial stage of crystallization, and the coercive force remains constant until the start of crystallization. The increase in magnesium-soft properties at this stage is explained by the presence of a single-axis anisotropy, which occurs according to Heyel-Taniguchi theory. During the crystallization process, both materials lose their magnetic soft properties.

Conflict of Interest

The authors declare that they have no conflicts of interest.

References

1. Kornienkov BA, Libman MA, Molotilov BV, Kadyshev DI (2015) Anomalous Magnetic Changes in Amorphous Fe–Ni–Si–B Alloy. Steel in Translation 45: 231-232.
2. Gruszka K, Nabialek M, Szota M (2016) Analysis of the thermal and magnetic properties of amorphous Fe61Co10Zr2.5 Hf2.5 Me2W2B20 (where Me Mo, Nb, Ni ORY) ribbons. Arch. Metall. Mater 61: 641-644.
3. Baicheng Zhang, Nour-Eddine Fenineche, Hanlin Liao, Christian Coddet (2013) Microstructure and Magnetic Properties of Fe Ni Alloy Fabricated by Selective Laser Melting Fe/Ni Mixed Powders. J. Mater. Sci. Technol 29: 757-760.
4. Chang CT, Shen BL, Inoue A (2006) Co-Fe-B-Si-Nb bulk glassy alloys with superh igh strength and extremely low magnetostriction. Appl Phys. Lett. 88: 011901-011903.
5. Suzuki K, Fujimori X, Hashimoto K (1987) amorphous metals. Ed. T. Masumoto. M. Metallurgy 1987: 150-156.

6. Inoue A, Shn BL (2002) Formation and soft magnetic properties of Co Fe-Si- B-Nb bulk glassy a llo)'S. 1\111/er: Trans 43: 1230-1234.
7. Nascimento L, Melnyk A (2017) Characterization of amorphous alloy Co87Nb46B15. J. Chil. Chem. Soc 62: 2.
8. Ahmadian Baghbaderani H, Sharafi S, Delshad Chermahini M (2012) Investigation of nanostructure formation mechanism and magnetic properties in Fe45Co45Ni10 system synthesized by mechanical alloying. Powder Technology 230: 241-246.
9. Bardzinskia PJ, Kopcewiczb M, Rybaczuka M, Mariusz Hasiak (2015) Magnetic Properties and Structure of Amorphous Fe74Hf4Ta1Cu1Gd1LaxSi15-xB4 (x=0; 7) Ribbons. ACTA PHYSICA POLONICA A 127: 827-830.
10. Babilasa R, Radona A, Gebara P (2017) Structure and Magnetic Properties of Fe–B–Si–Zr Metallic Glasses. ACTA PHYSICA POLONICA A 131: 726-728.